

Antiferromagnetic behavior in single-wall carbon nanotubes

V. Likodimos,¹ S. Glenis,¹ N. Guskos,¹ and C. L. Lin²

¹*Department of Physics, University of Athens, Panepistimiopolis, Zografou, Athens 15784, Greece*

²*Department of Physics, Temple University, Philadelphia, Pennsylvania 19122, USA*

(Received 17 January 2007; revised manuscript received 4 April 2007; published 15 August 2007)

The electronic properties of single-wall carbon nanotubes (SWNTs) have been studied using dc magnetization and electron spin resonance (ESR). The dc magnetization displays a weak diamagnetic susceptibility of $\approx 10^{-7}$ emu/g. ESR measurements reveal a narrow resonance line of low intensity and metallic line shape. The spin susceptibility shows a major Pauli contribution at high temperatures ($T > 150$ K) and an appreciable Curie component at lower temperatures. A marked drop of the spin susceptibility is observed at $T < 14$ K, pointing to the opening of a spin gap at low temperatures. The underlying mechanism is discussed in terms of an electronic instability of the SWNTs or the occurrence of defect-mediated spin magnetism.

DOI: [10.1103/PhysRevB.76.075420](https://doi.org/10.1103/PhysRevB.76.075420)

PACS number(s): 81.07.De, 73.63.Fg, 75.75.+a, 76.30.Pk

I. INTRODUCTION

Carbon nanotubes (CNs) have emerged as a unique class of low dimensional materials with exceptional electronic properties and tunability that hold promise for the development of nanoelectronics.¹ Single-wall carbon nanotubes (SWNTs) represent a close realization of one-dimensional (1D) conductors with strong electron-electron interactions providing access to the low-energy properties of strongly correlated mesoscopic systems, the most notable aspect being the Luttinger-liquid (LL) state driven by the Coulomb repulsion of 1D electrons,² evidenced in electrical transport^{3,4} and photoemission^{5,6} measurements. Experimental observations of superconductivity in SWNT ropes⁷ and ultrathin SWNTs (Ref. 8) have generated further interest in the interplay of the long-range Coulomb interactions with electron-phonon coupling and the electrostatic screening due to intertube coupling that may account for the growth of superconducting correlations or a charge density wave instability.⁹ Recently, nuclear magnetic resonance (NMR) experiments on ¹³C enriched double-wall CNs revealed the formation of a gap in the spin excitation spectrum below 20 K,¹⁰ pointing out the rich variety of electronic instabilities that may arise in the 1D CN structure.

In spite of the high perfection and robustness of the SWNT's structure, the presence of low amounts of disorder due to defects and imperfections has been found to modify substantially electronic transport in nanotube devices.¹¹ Moreover, theoretical studies have shown that structural defects such as vacancies and adatoms may acquire spin polarization depending on the tube radius and chirality,¹² while the formation of localized edge states in heterostructured C/BN nanotubes¹³ and finite length CNs with noncompensated zigzag open ends¹⁴ has also been predicted to promote magnetism. Electron spin resonance (ESR) is a suitable probe of spin dynamics in low dimensional metallic systems. Its sensitivity on both localized and itinerant spins has been exploited to study the variation of the electronic properties of multiwall CNs (MWNTs) caused by the confined CN geometry and the acceptor action of structural defects in pristine materials,¹⁵⁻¹⁸ chemical doping that leads to Fermi level shifts and quasibound localized states,^{19,20} and electron irradiation.²¹

However, the use of ESR in SWNTs has been severely obstructed by the presence of residual ferromagnetic catalyst particles, practically absent in MWNTs grown by the non-catalytic arc-discharge method. In particular, ESR has been observed in high quality crystalline ropes of SWNTs soon after the implementation of their high-yield synthesis by the laser vaporization technique, providing evidence for intrinsically metallic behavior.^{22,23} Despite the long spin relaxation time anticipated in the 1D tube structure that would lead to a rather narrow conduction electron spin resonance (CESR), as well as theoretical predictions of a fine structure in the CESR spectrum related to the spin-charge separation of the LL state,²⁴ subsequent studies of SWNTs systematically noted the absence of CESR²⁵⁻²⁷ which, however, was restored upon electrochemical K doping.²⁶ These diverse observations can be reconciled with an excessive increase of the spin relaxation rate in undoped SWNTs by the strong spin-flip scattering of conduction electrons on metallic impurities because of their long spin diffusion length that renders ESR undetectable.²⁶ More recently, a weak ESR line has been reported in pristine SWNTs with no Pauli contribution in the spin susceptibility, which intensified upon electron irradiation and followed a thermally deactivated behavior, associated with localized states in semiconducting SWNTs interacting with metallic impurities.²⁸

In this work, we report on the observation of a narrow ESR line of weak intensity and metallic line shape in pristine samples consisting of SWNT bundles, whose dc magnetization shows a weak diamagnetic susceptibility superimposed on the strong ferromagnetic response of residual catalyst particles. The spin susceptibility of the narrow ESR line varies slowly down to low temperatures, following the exchange coupling model of conduction electrons and localized spins. However, a sharp drop of the spin susceptibility is observed at $T < 14$ K. This indicates the opening of a spin gap at low temperatures, which is discussed in terms of an electronic instability of the SWNTs or the presence of defect-mediated spin magnetism.

II. EXPERIMENTAL DETAILS

Experiments were performed on SWNT samples prepared by the laser oven vaporization technique in Rice Univer-

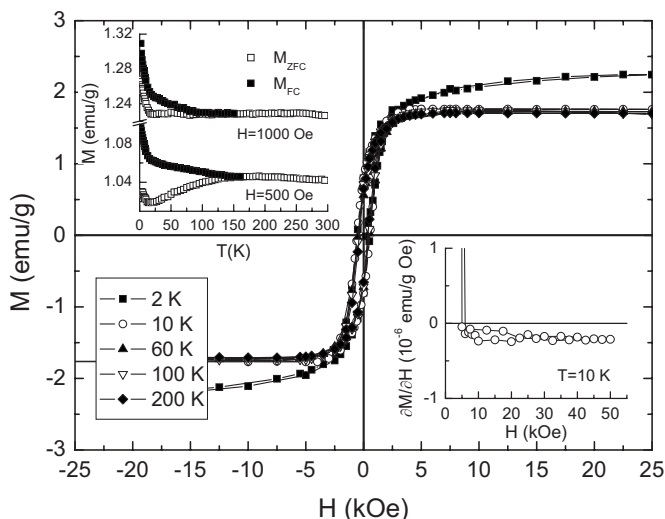


FIG. 1. Magnetization loops of SWNTs at different temperatures. The upper inset shows the temperature dependence of the dc magnetization at 500 and 1000 Oe. The lower inset shows the field dependence of the differential susceptibility $\partial M / \partial H$ at 10 K.

sity.²² Characterization by x-ray diffraction and transmission electron microscopy confirmed the aggregated morphology of the specimens consisting of self-assembled bundles or ropes of SWNTs, with small amounts of catalyst (Ni, Co) particles. The ropes are several micrometers long, with diameter varying between 10 and 85 nm, and form a two-dimensional triangular lattice with a lattice constant of 1.7 nm. To characterize the dc magnetic response, magnetization measurements were carried out using a Quantum Design MPMS superconducting quantum interference device magnetometer on specimens obtained after filtration of a SWNT suspension in toluene, where the pristine specimens were stored. ESR measurements were performed on a conventional X-band spectrometer ($\nu \approx 9.42$ GHz) with a continuous flow cryostat for temperature-dependent measurements (4–300 K). The magnetic field was scaled with a NMR gaussmeter, while the g factor and ESR intensity were measured with respect to standard calibration samples.

III. RESULTS AND DISCUSSION

Figure 1 summarizes the dc magnetic measurements of the SWNT bundles. The dc magnetic response is determined by the contribution of ferromagnetic (Ni, Co) catalyst residues causing the appearance of hysteresis loops with coercive field varying between 560 and 370 Oe as temperature increases from 2 to 200 K. The temperature dependence of the dc magnetization $M(T)$ in the zero-field cooled (ZFC) and field cooled (FC) modes shows significant irreversibility and a broad maximum at low magnetic fields (upper inset of Fig. 1), characteristic of a large size distribution of ferromagnetic nanoparticles with an average blocking temperature of 190 K at $H=500$ Oe, while the increase of both M_{ZFC} and M_{FC} branches at $T < 10$ K indicates the presence of a small fraction of unblocked nanoparticles. The field derivative of the isothermal $M(H)$ up to 50 kOe reveals a rather

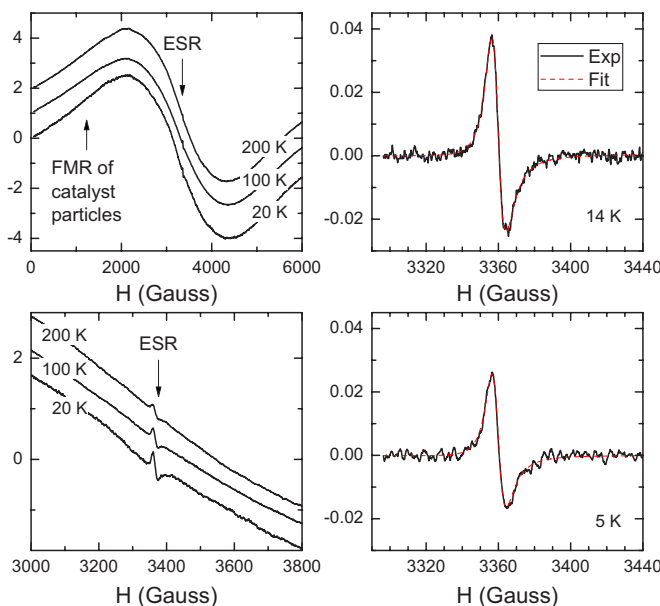


FIG. 2. (Color online) ESR spectra of the SWNTs at various temperatures and magnetic field scans. Arrows in the larger field scans (left panels) point out the narrow ESR line superimposed on the FMR of the catalyst particles. Thin dashed lines in the small scan spectra (right panels) show the best fit metallic line shapes at 5 and 14 K after subtraction of the ferromagnetic background.

small field-independent contribution of the order of -2×10^{-7} emu/g, which is much lower than that of pristine MWNTs (Refs. 18 and 29) and comparable to that of B-doped MWNTs,²⁰ where the Fermi level shift of ~ 0.2 eV causes the suppression of the pronounced orbital diamagnetism of graphite.^{30,31} Recent magnetic-field-dependent photoluminescence experiments on surfactant isolated SWNTs revealed a diamagnetic anisotropy of the order of -1×10^{-6} emu/g for semiconducting CNs,^{32,33} in agreement with theoretical predictions.^{34,35} The small diamagnetic susceptibility observed in the SWNT bundles may then be associated with the contribution of metallic CNs, which are predicted to be paramagnetic along the tube axis, and most likely with the presence of defects leading to the effective doping of the CN structure, where slight shifts of the Fermi level may drastically reduce the diamagnetic susceptibility.^{34–36}

Figure 2 shows representative ESR spectra of the SWNT specimens at different temperatures and successively smaller magnetic field scan ranges. A broad resonance signal at $g=2.15$ due to the ferromagnetic catalyst particles dominates the ESR spectra, which varies weakly with temperature in agreement with the dc magnetic response. However, a narrow ESR line superimposed on the broad ferromagnetic signal, a small trace of it can be hardly discerned in the large field scan, is successively resolved upon zooming in the $g=2.0$ region. After subtraction of the ferromagnetic background, which, in the small field scan of 150 G, can be accurately fitted by a polynomial base line, the narrow ESR signal exhibits an asymmetric line shape (right panels of Fig. 2). This line shape is typical of conducting samples when the sample thickness is comparable to the skin depth, where the

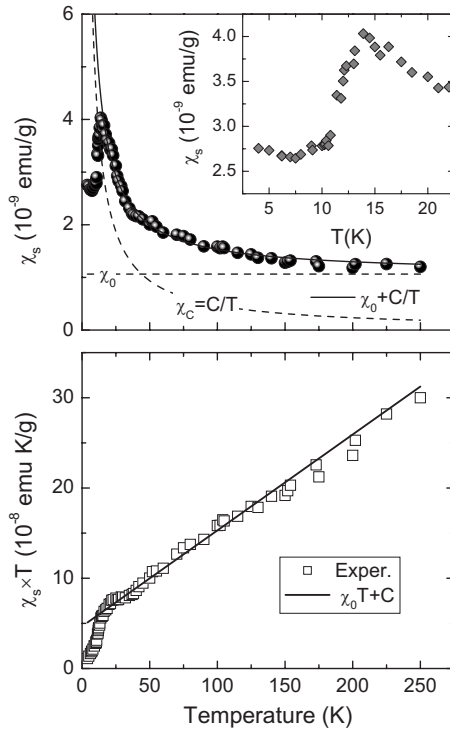


FIG. 3. Temperature dependence of the spin susceptibility χ_s and $\chi_s T$ for the SWNTs. Solid and dashed lines depict the decomposition of $\chi_s(T)$ to a constant Pauli term χ_0 and a Curie $\chi_C=C/T$ contribution. The inset shows in detail the low-temperature variation of $\chi_s(T)$.

skin effect drives electric and magnetic components of the rf field out of phase leading to the admixture of dispersion (χ') into the absorption (χ'') spectra.³⁷ The ESR line has been accordingly fitted to the line shape³⁸

$$\frac{d\chi}{dH} = \left(\frac{\cos \phi}{\Delta H^2} \right) \frac{-2y + (1 - y^2)\tan \phi}{(1 + y^2)^2}, \quad (1)$$

where $y=(H-H_0)/\Delta H$, with H_0 being the resonance field and ΔH the half-width at half-height, while $\tan \phi=\alpha$ is the ratio of dispersion to absorption ($\chi=\chi'' \cos \phi + \chi' \sin \phi$). The asymmetry parameter varies between the values $\alpha=0$ ($\phi=0$) that gives a symmetric Lorentzian line and $\alpha=1$ ($\phi=\pi/4$) that produces an asymmetric resonance line with absorption and dispersion at equal weight, corresponding to the classical asymmetry ratio $A/B=2.55$ of the CESR line shape for a thick metallic sample.³⁷ The narrow ESR line can be well fitted to this single metallic line shape, as shown by the dashed lines in the right panels of Fig. 2.

Figure 3 shows the temperature dependence of the spin susceptibility $\chi_s(T)$ and the corresponding product $\chi_s T$ for the narrow ESR line. To account for the temperature variation of the skin depth, χ_s was determined from the area under the integrated absorption component ($d\chi''/dH$) of the ESR spectra derived from fitting to Eq. (1), after being corrected for the inhomogeneous phase of the microwave field through the $\cos \phi$ factor. The spin susceptibility is nearly constant down to 150 K, followed by a moderate increase at lower

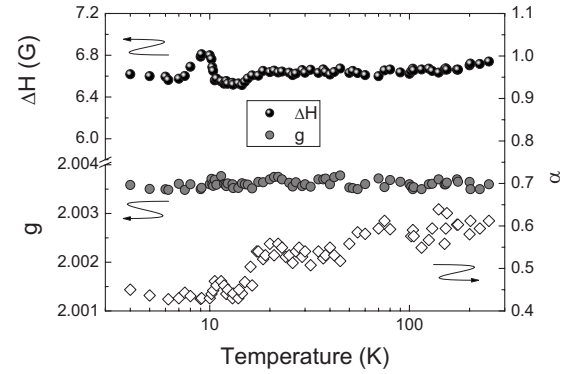


FIG. 4. Temperature dependence of the linewidth ΔH , g factor, and the asymmetry parameter α for the narrow ESR line of the SWNTs.

temperatures. This temperature variation complies with the strong exchange coupling of conduction electrons and localized spins that leads to a single ESR line. In this case, the spin susceptibility becomes $\chi_s=\chi_0+\chi_C$ stemming from the superposition of a temperature-independent (Pauli) term χ_0 that is dominant at high temperatures and a Curie contribution $\chi_C=C/T$ arising from the susceptibility of localized spins that causes the gradual upturn of $\chi_s(T)$ at lower temperatures. Such a behavior can be more conveniently identified in the temperature dependence of $\chi_s T$ that varies over a broad temperature range according to $\chi_0 T+C$, as shown in the lower panel of Fig. 3. An effective description of $\chi_s(T)$ is thus derived down to 15 K with $\chi_0=1.06(3) \times 10^{-9}$ emu/g and $C=4.7(1) \times 10^{-8}$ emu K/g corresponding to a density of localized spins of 7.5×10^{16} spins/g. The value of χ_0 is considerably lower than that of MWNTs, where $\chi_0 \approx 7 \times 10^{-9}$ emu/g,^{16,18} implying that only a fraction of tubes contributes to the ESR signal, whereas the concentration of localized spins is of comparable magnitude to that of pristine paramagnetic defects in MWNTs.^{16,18,20} Most importantly, the spin susceptibility decreases rapidly below 14 K, decaying exponentially down to about 7 K below which a slight upturn of χ_s is observed (inset of Fig. 3). This steep drop of $\chi_s(T)$ is reminiscent of the thermally activated spin susceptibility of 1D systems with a spin gap of the order of the χ_s maximum temperature.^{39,40} However, in the present case, χ_s does not tend to zero at lower temperatures but nearly saturates at a value exceeding considerably the high-temperature susceptibility without showing any pronounced paramagnetic Curie tail.

Figure 4 shows the temperature dependence of the ESR linewidth ΔH , g factor, and the asymmetry parameter α of the ESR line. The g factor remains approximately constant at 2.0035 as a function of temperature. Likewise, $\Delta H(T)$ and $\alpha(T)$, the latter being an increasing function of the electrical conductivity, do not vary appreciably with temperature down to 20 K. According to Elliott's mechanism, a dominant contribution to the spin-lattice relaxation rate arises from spin-orbit scattering on phonons, which, being proportional to the momentum relaxation rate, leads to a linear $\Delta H(T)$ variation that scales with the electrical resistivity.⁴¹ Moreover, spin-lattice relaxation can be significantly impeded in 1D metals

by the limitation in momentum space into which electrons can scatter and relax efficiently.⁴² The absence of a linear $\Delta H(T)$ dependence in the SWNT bundles may then be brought up by the weak electron-phonon scattering reflected in the suppressed variation of $\alpha(T)$, and the strong coupling of conduction electrons to localized spins, characterized by a temperature-independent relaxation rate. However, a small anomaly of $\Delta H(T)$ is traced below 20 K, while a decrease of the asymmetry parameter α is resolved at the same temperature range, indicative of a reduction of the sample's conductivity that correlates with the low-temperature peak of $\chi_s(T)$.

This behavior resembles to some extent ESR in quasi-1D organic conductors, where a steep drop of $\chi_s(T)$ and an anomalous variation of $\Delta H(T)$ are typical features of spin density or charge density wave instabilities that lead to an insulating antiferromagnetic ground state.^{40,43} In addition, the anomalous behavior of $\chi_s(T)$ occurs at the same energy scale ($T < 20$ K), where the formation of a spin gap ($2\Delta \approx 40$ K) was derived from the suppression of the ¹³C NMR relaxation rate in double-wall CNs.¹⁰ An electronic instability of the SWNT's ground state causing the opening of a gap in the spin excitation spectrum may be accordingly suggested to explain the sharp decrease of χ_s below 14 K, in accordance with theoretical predictions for the effects of electron-electron interactions in SWNTs.^{2,9} On the other hand, despite the bulklike reduction of the conductivity inferred from the decrease of $\alpha(T)$, the persistence of considerable spin density below the peak of $\chi_s(T)$ as well as the small kink of $\Delta H(T)$, which is expected to diverge at the antiferromagnetic transition temperature, do not definitely determine the presence of magnetic ordering.

Relying on the relatively high contribution of localized spins to the total spin susceptibility at $T < 30$ K (Fig. 3), a defect-driven mechanism may be alternatively invoked to account for the low-temperature peak of $\chi_s(T)$. In particular, the presence of antiferromagnetic exchange coupling be-

tween the localized spin moments, as indicated by the downturn of $\chi_s T$ at low temperatures (Fig. 3), might also explain the low-temperature anomaly of the spin susceptibility. However, the low spin concentration of paramagnetic defects deduced from the Curie component of χ_s precludes ordinary localized spin magnetism. In this case, the exchange interactions between the localized spins should be mediated by the conduction electrons, as recently suggested for activated carbon fibers consisting of a disordered network of nanographites⁴⁴ and carbon nanohorns,⁴⁵ where the spin susceptibility exhibits similar cusps in the temperature regime of 4–17 K. Furthermore, recent theoretical work has predicted substantial magnetic interactions between spin polarized edge states in graphitic fragments,⁴⁶ and most importantly that localized states induced by vacancies in graphene may spread over many lattice sites in the presence of a finite impurity concentration.⁴⁷ The latter might then provide a possible mechanism for the coupling of localized and itinerant spins in some defective SWNTs causing the low-temperature anomaly in the spin susceptibility.

IV. CONCLUSIONS

In conclusion, ESR measurements on bundles of SWNTs allow to single out a narrow resonance line of weak intensity and metallic line shape, superimposed on the strong ferromagnetic resonance (FMR) of the residual catalyst particles. The temperature dependence of the spin susceptibility is compatible with the exchange coupling of conduction electrons and localized spins, with a major metallic Pauli contribution at $T > 150$ K. Most notably, a drastic reduction of the spin susceptibility is observed at $T < 14$ K, accompanied by a decrease of the electrical conductivity. This behavior suggests the opening of a spin gap, which is discussed in terms of an electronic instability toward an antiferromagnetic insulating ground state due to electron-electron interactions or a defect-driven magnetic effect due to the antiferromagnetic coupling of localized spins mediated by the conduction carriers.

¹M. S. Dresselhaus, G. Dresselhaus, and Ph. Avouris, *Carbon Nanotubes: Synthesis, Structure, Properties, and Applications* (Springer, Berlin, 2001); M. P. Anantram and F. Léonard, *Rep. Prog. Phys.* **69**, 507 (2006).

²R. Egger and A. O. Gogolin, *Phys. Rev. Lett.* **79**, 5082 (1997); *Eur. Phys. J. B* **3**, 281 (1998); C. Kane, L. Balents, and M. P. A. Fisher, *Phys. Rev. Lett.* **79**, 5086 (1997); H. Yoshioka and A. A. Odintsov, *ibid.* **82**, 374 (1999).

³M. Bockrath, D. H. Cobden, J. Lu, A. G. Rinzler, R. E. Smalley, L. Balents, and P. L. McEuen, *Nature (London)* **397**, 598 (1999).

⁴Z. Yao, H. W. Ch. Postma, L. Balents, and C. Dekker, *Nature (London)* **402**, 273 (1999).

⁵H. Ishii *et al.*, *Nature (London)* **426**, 540 (2003).

⁶H. Rauf, T. Pichler, M. Knupfer, J. Fink, and H. Kataura, *Phys. Rev. Lett.* **93**, 096805 (2004).

⁷M. Kociak, A. Yu. Kasumov, S. Guéron, B. Reulet, I. I. Khodos, Yu. B. Gorbatov, V. T. Volkov, L. Vaccarini, and H. Bouchiat,

Phys. Rev. Lett. **86**, 2416 (2001).

⁸Z. K. Tang, L. Zhang, N. Wang, X. X. Zhang, G. H. Wen, G. D. Li, J. N. Wang, C. T. Chan, and P. Sheng, *Science* **292**, 2462 (2001).

⁹O. Dubay, G. Kresse, and H. Kuzmany, *Phys. Rev. Lett.* **88**, 235506 (2002); A. De Martino and R. Egger, *Phys. Rev. B* **67**, 235418 (2003); J. González and J. V. Alvarez, *ibid.* **70**, 045410 (2004); R. Barnett, E. Demler, and E. Kaxiras, *ibid.* **71**, 035429 (2005).

¹⁰P. M. Singer, P. Wzietek, H. Alloul, F. Simon, and H. Kuzmany, *Phys. Rev. Lett.* **95**, 236403 (2005).

¹¹M. Bockrath, W. Liang, D. Bozovic, J. H. Hafner, C. M. Lieber, M. Tinkham, and H. Park, *Science* **291**, 283 (2001); M. Freitag, A. T. Johnson, S. V. Kalinin, and D. A. Bonnell, *Phys. Rev. Lett.* **89**, 216801 (2002); C. Gómez-Navarro, P. J. de Pablo, J. Gómez-Herrero, B. Biel, F. J. Garcia-Vidal, A. Rubio, and F. Flores, *Nat. Mater.* **4**, 534 (2005); Y. Fan, B. R. Goldsmith, and P. G. Collins, *ibid.* **4**, 906 (2005).

- ¹²P. O. Lehtinen, A. S. Foster, A. Ayuela, T. T. Vehviläinen, and R. M. Nieminen, *Phys. Rev. B* **69**, 155422 (2004); Y. Ma, P. O. Lehtinen, A. S. Foster, and R. M. Nieminen, *New J. Phys.* **6**, 68 (2004).
- ¹³J. Choi, Y.-H. Kim, K. J. Chang, and D. Tománek, *Phys. Rev. B* **67**, 125421 (2003).
- ¹⁴S. Okada and A. Oshiyama, *J. Phys. Soc. Jpn.* **72**, 1510 (2003).
- ¹⁵M. Kosaka, T. W. Ebbesen, H. Hiura, and K. Tanigaki, *Chem. Phys. Lett.* **225**, 161 (1994); **233**, 47 (1995).
- ¹⁶O. Chauvet, L. Forró, W. Bacsá, D. Ugarte, B. Doudin, and W. A. de Heer, *Phys. Rev. B* **52**, R6963 (1995).
- ¹⁷A. S. Kotosonov and D. V. Shilo, *Carbon* **36**, 1649 (1998).
- ¹⁸V. Likodimos, S. Glenis, N. Guskos, and C. L. Lin, *Phys. Rev. B* **68**, 045417 (2003).
- ¹⁹O. Chauvet, G. Baumgartner, M. Carrard, W. Bacsá, D. Ugarte, W. A. de Heer, and L. Forró, *Phys. Rev. B* **53**, 13996 (1996).
- ²⁰V. Likodimos, S. Glenis, and C. L. Lin, *Phys. Rev. B* **72**, 045436 (2005).
- ²¹F. Beuneu, C. L'Huillier, J.-P. Salvetat, J.-M. Bonard, and L. Forró, *Phys. Rev. B* **59**, 5945 (1999).
- ²²A. Thess *et al.*, *Science* **273**, 483 (1996).
- ²³P. Petit, E. Jouguelet, J. E. Fischer, A. G. Rinzler, and R. E. Smalley, *Phys. Rev. B* **56**, 9275 (1997).
- ²⁴A. De Martino, R. Egger, K. Hallberg, and C. A. Balseiro, *Phys. Rev. Lett.* **88**, 206402 (2002).
- ²⁵S. Bandow, S. Asaka, X. Zhao, and Y. Ando, *Appl. Phys. A: Mater. Sci. Process.* **67**, 23 (1998).
- ²⁶A. S. Claye, N. M. Nemes, A. Jánosy, and J. E. Fischer, *Phys. Rev. B* **62**, R4845 (2000).
- ²⁷K. Shen, D. L. Tierney, and T. Pietraß, *Phys. Rev. B* **68**, 165418 (2003).
- ²⁸J.-P. Salvetat, T. Fehér, C. L'Huillier, F. Beuneu, and L. Forró, *Phys. Rev. B* **72**, 075440 (2005).
- ²⁹A. S. Kotosonov, *Pis'ma Zh. Eksp. Teor. Fiz.* **70**, 476 (1999) [*JETP Lett.* **70**, 476 (1999)].
- ³⁰M. S. Dresselhaus and G. Dresselhaus, *Adv. Phys.* **30**, 139 (1981).
- ³¹A. S. Kotosonov, *Pis'ma Zh. Eksp. Teor. Fiz.* **43**, 30 (1986) [*JETP Lett.* **43**, 37 (1986)].
- ³²S. Zaric, G. N. Ostojic, J. Kono, J. Shaver, V. C. Moore, R. H. Hauge, R. E. Smalley, and X. Wei, *Nano Lett.* **4**, 2219 (2004).
- ³³O. N. Torrens, D. E. Milkie, H. Y. Ban, M. Zheng, G. B. Onoa, T. D. Gierke, and J. M. Kikkawa, *J. Am. Chem. Soc.* **129**, 253 (2007).
- ³⁴H. Ajiki and T. Ando, *J. Phys. Soc. Jpn.* **64**, 4382 (1995).
- ³⁵J. P. Lu, *Phys. Rev. Lett.* **74**, 1123 (1995).
- ³⁶A. S. Kotosonov and V. V. Atrazhev, *Pis'ma Zh. Eksp. Teor. Fiz.* **72**, 76 (2000) [*JETP Lett.* **72**, 53 (2000)].
- ³⁷G. Feher and A. F. Kip, *Phys. Rev.* **98**, 337 (1955); J. Pifer and R. Magno, *Phys. Rev. B* **3**, 663 (1971).
- ³⁸V. Sitaram, A. Sharma, S. V. Bhat, K. Mizoguchi, and R. Menon, *Phys. Rev. B* **72**, 035209 (2005).
- ³⁹D. C. Johnston, *Phys. Rev. Lett.* **52**, 2049 (1984); D. C. Johnston, R. K. Kremer, M. Troyer, X. Wang, A. Klümper, S. L. Bud'ko, A. F. Panchula, and P. C. Canfield, *Phys. Rev. B* **61**, 9558 (2000).
- ⁴⁰M. Dumm, A. Loidl, B. W. Fravel, K. P. Starkey, L. K. Montgomery, and M. Dressel, *Phys. Rev. B* **61**, 511 (2000).
- ⁴¹R. J. Elliott, *Phys. Rev.* **96**, 266 (1954); Y. Yafet, *Solid State Phys.* **14**, 1 (1963).
- ⁴²L. Forró and C. Schönenberger, in *Carbon Nanotubes*, edited by M. S. Dresselhaus, G. Dresselhaus, and Ph. Avouris (Springer, Berlin, 2001).
- ⁴³Y. Tomkiewicz, *Phys. Rev. B* **19**, 4038 (1979); H. J. Pedersen, J. C. Scott, and K. Bechgaard, *ibid.* **24**, 5014 (1981).
- ⁴⁴Y. Shibayama, H. Sato, T. Enoki, and M. Endo, *Phys. Rev. Lett.* **84**, 1744 (2000).
- ⁴⁵S. Garaj, L. Thien-Nga, R. Gaal, L. Forró, K. Takahashi, F. Kokai, M. Yudasaka, and S. Iijima, *Phys. Rev. B* **62**, 17 115 (2000).
- ⁴⁶H. Lee, Y.-W. Son, N. Park, S. Han, and J. Yu, *Phys. Rev. B* **72**, 174431 (2005).
- ⁴⁷V. M. Pereira, F. Guinea, J. M. B. Lopes dos Santos, N. M. R. Peres, and A. H. Castro Neto, *Phys. Rev. Lett.* **96**, 036801 (2006).